International Journal of Engineering and Advanced Technology (IJEAT)
ISSN: 2249-8958 (Online), Volume-7 Issue-1, October 2017

Dynamic Analysis of Structures using a Solid-Shell Element

Cengiz POLAT

Abstract: ***Dynamic analysis of some structures are performed using a solid-shell element. An eight node solid-shell element is used in the analyses. The Assumed Natural Strain (ANS) and the Enhanced Assumed Strain (EAS) methods are used to alleviate the locking problems. The governing equations are solved employing the Newmark's integration technique. Several benchmark problems are solved to demonstrate the efficiency of the element.***

Keywords: Solid-shell element; ANS-EAS method, Dynamic Analysis.

I. INTRODUCTION

Dynamic analysis of plates and shells has been studied widely because of their extensive applications. In the linear analysis, the displacements and strains developed in the structure are small. That is, the geometry of the structure assumed remains unchanged during the loading process and linear strain approximations can be used [1]. Many researchers [2-10] are interested in solid-shell elements which are widely used to analyze shell like structures. These elements possess no rotational degrees-of-freedom. Thus, the complication on handling finite rotational increments can be avoided. However, similar to the degenerated shell elements these elements also suffer from some kind of locking effects. Various methods have been suggested to overcome these locking effects. The earliest techniques are Uniform Reduced Integration (URI) [11] and Selective Reduced Integration (SRI) [12]. However, URI procedure generally leads to spurious zero energy modes, despite the fact that for some cases a correct solution is obtained. In addition, SRI procedure exhibits similar problems but usually on a smaller range. Another two distinct approaches are the Assumed Natural Strain (ANS) [13] and the Enhanced Assumed Strain (EAS) [14] which are successfully implemented in various finite elements to alleviate locking effects. The aim of this paper is to establish the nearly locking free formulation of an 8-node solid-shell element and its applications to dynamic problems. Firstly, the geometry and the strain-displacement relations of the displacement based 8-node solid-shell element are demonstrated. Low order elements based on standard displacement interpolation are usually accompanied by locking phenomena. To alleviate the transverse shear and trapezoidal locking problems of the element, the ANS approach is used.

Manuscript published on 30 October 2017.
* Correspondence Author (s)
Cengiz POLAT*, Firat University, Technical Vocational School, Elazig, TURKEY. E-mail: cpolat@firat.edu.tr

In addition, membrane and thickness locking treatments are done by the EAS method. The EAS method is based on the enhancing of the displacement-dependent strain field by an extra assumed strain field, And it is assumed that the stress and the enhanced assumed strain fields are orthogonal, which results in an elimination of the stress field from the finite element equations. Secondly, a brief algorithm for dynamic analyses is given. Lastly, several benchmark problems are examined by a computer program which is written by the author in MATLAB code.

II. ELEMENT FORMULATION

2.1. Geometry of the Solid Shell Element

The coordinates of a typical point in the eight node solid-shell element (Fig. 1.) can be written as

$$\mathbf{x}=\sum_{k=1}^{4} N_k\left(\frac{1+\zeta}{2}\mathbf{x}_k^t+\frac{1-\zeta}{2}\mathbf{x}_k^b\right) \qquad (1)$$

where $N_k = N_k(\xi,\eta)$ are the two-dimensional isoperimetric shape functions, $\mathbf{x}=[x,y,z]^T$ are the position vectors; ξ, η and ζ are curvilinear coordinates. Here ξ, η and ζ are assumed to vary from -1 and +1.

The displacement field $\mathbf{u}=[u,v,w]^T$ in the shell element can be approximated by

$$\mathbf{u}=\sum_{k=1}^{4} N_k\left(\frac{1+\zeta}{2}\mathbf{u}_k^t+\frac{1-\zeta}{2}\mathbf{u}_k^b\right) \qquad (2)$$

where $\mathbf{u}_k=[u_k,v_k,w_k]^T$ represents the displacement vector of node k.

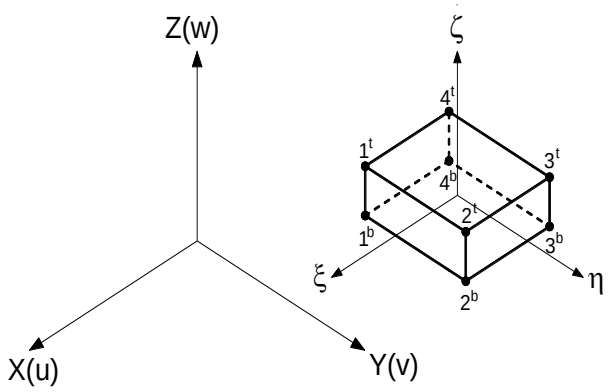

Figure 1. Geometry of the eight node solid-shell element.

Published By:
Blue Eyes Intelligence Engineering
and Sciences Publication (BEIESP)

2.2. Strain–Displacement Relationships

The components of the displacement-based strain tensor $\boldsymbol{\varepsilon}^{u}$ in the natural set of coordinates (ξ,η,ζ) can be given as

$$\boldsymbol{\varepsilon}^{u}=[\varepsilon^{u}_{\xi\xi}\quad\varepsilon^{u}_{\eta\eta}\quad\varepsilon^{u}_{\zeta\zeta}\quad\varepsilon^{u}_{\xi\eta}\quad\varepsilon^{u}_{\xi\zeta}\quad\varepsilon^{u}_{\eta\zeta}]^{T} \tag{3}$$

or

$$\boldsymbol{\varepsilon}^{u}=\mathbf{B}^{u}\,\mathbf{u},\ \mathbf{u}=[\mathbf{u}_{1}\quad .\quad .\quad .\quad \mathbf{u}_{k}]^{T}\ k=1,...n \tag{4}$$

where $\mathbf{B}^{u}$ is the conventional strain-displacement matrix and $\mathbf{u}$ is the nodal displacement vector. The natural strain components defined in Eq. (3) can be determined by using the displacement vector $\mathbf{u}$ and the covariant base vectors $\mathbf{g}_{i}$ as

$$\varepsilon^{u}_{\xi_i\xi_j}=\frac{1}{2}\left(\frac{\partial\mathbf{u}}{\partial\xi_i}\mathbf{g}_j+\frac{\partial\mathbf{u}}{\partial\xi_j}\mathbf{g}_i\right)\ (i,j=1,2,3;\ \xi_1=\xi,\ \xi_2=\eta,\ \xi_3=\zeta) \tag{5}$$

and

$$\mathbf{g}_{i}=\frac{\partial\mathbf{x}}{\partial\xi_{i}} \tag{6}$$

where $\mathbf{x}$ is the position vector [15,16].

The previously described strain field is related to the natural set of coordinates. Therefore, it is necessary to obtain the local physical strains from the natural strain components. An algorithm suggested by Valente [17] is used for the transformation of the strains. It consists of the following five steps:

a) $\mathbf{r}^{3}=\left[\frac{\partial x}{\partial\xi}\quad\frac{\partial y}{\partial\xi}\quad\frac{\partial z}{\partial\xi}\right]^{T}\times\left[\frac{\partial x}{\partial\eta}\quad\frac{\partial y}{\partial\eta}\quad\frac{\partial z}{\partial\eta}\right]^{T}$

b) $\mathbf{r}^{3}=\frac{\mathbf{r}^{3}}{\|\mathbf{r}^{3}\|}$

c) $\mathbf{r}^{1}=\left[\frac{\partial x}{\partial\xi}\quad\frac{\partial y}{\partial\xi}\quad\frac{\partial z}{\partial\xi}\right]^{T}$

d) $\mathbf{r}^{1}=\frac{\mathbf{r}^{1}}{\|\mathbf{r}^{1}\|}$

e) $\mathbf{r}^{2}=\mathbf{r}^{3}\times\mathbf{r}^{1}$

Then, the components of director cosines matrix $\hat{\mathbf{T}}$ is

$$\hat{\mathbf{T}}=\left[\mathbf{r}^{1}\quad\mathbf{r}^{2}\quad\mathbf{r}^{3}\right]^{T}(\mathbf{J})^{-1} \tag{7}$$

in which $\mathbf{J}$ is the conventional Jacobian matrix given by

$$\mathbf{J}=\begin{bmatrix}\frac{\partial x}{\partial\xi}&\frac{\partial y}{\partial\xi}&\frac{\partial z}{\partial\xi}\\ \frac{\partial x}{\partial\eta}&\frac{\partial y}{\partial\eta}&\frac{\partial z}{\partial\eta}\\ \frac{\partial x}{\partial\zeta}&\frac{\partial y}{\partial\zeta}&\frac{\partial z}{\partial\zeta}\end{bmatrix} \tag{8}$$

The natural coordinate and the local coordinate system can be related by the second-order transformation tensor $\overline{\mathbf{T}}$

$$\overline{\mathbf{T}}=\begin{bmatrix}\hat{T}_{11}\hat{T}_{11}&\hat{T}_{12}\hat{T}_{12}&\hat{T}_{13}\hat{T}_{13}&\hat{T}_{11}\hat{T}_{12}&\hat{T}_{11}\hat{T}_{13}&\hat{T}_{12}\hat{T}_{13}\\ \hat{T}_{21}\hat{T}_{21}&\hat{T}_{22}\hat{T}_{22}&\hat{T}_{23}\hat{T}_{23}&\hat{T}_{21}\hat{T}_{22}&\hat{T}_{21}\hat{T}_{23}&\hat{T}_{22}\hat{T}_{23}\\ \hat{T}_{31}\hat{T}_{31}&\hat{T}_{32}\hat{T}_{32}&\hat{T}_{33}\hat{T}_{33}&\hat{T}_{31}\hat{T}_{32}&\hat{T}_{31}\hat{T}_{33}&\hat{T}_{32}\hat{T}_{33}\\ 2\hat{T}_{11}\hat{T}_{21}&2\hat{T}_{12}\hat{T}_{22}&2\hat{T}_{13}\hat{T}_{23}&\hat{T}_{11}\hat{T}_{22}+\hat{T}_{12}\hat{T}_{21}&\hat{T}_{11}\hat{T}_{23}+\hat{T}_{21}\hat{T}_{13}&\hat{T}_{12}\hat{T}_{23}+\hat{T}_{22}\hat{T}_{13}\\ 2\hat{T}_{11}\hat{T}_{31}&2\hat{T}_{12}\hat{T}_{32}&2\hat{T}_{13}\hat{T}_{33}&\hat{T}_{11}\hat{T}_{32}+\hat{T}_{12}\hat{T}_{31}&\hat{T}_{11}\hat{T}_{33}+\hat{T}_{31}\hat{T}_{13}&\hat{T}_{12}\hat{T}_{33}+\hat{T}_{32}\hat{T}_{13}\\ 2\hat{T}_{21}\hat{T}_{31}&2\hat{T}_{22}\hat{T}_{32}&2\hat{T}_{23}\hat{T}_{33}&\hat{T}_{21}\hat{T}_{32}+\hat{T}_{22}\hat{T}_{31}&\hat{T}_{21}\hat{T}_{33}+\hat{T}_{31}\hat{T}_{23}&\hat{T}_{22}\hat{T}_{33}+\hat{T}_{32}\hat{T}_{23}\end{bmatrix} \tag{9}$$

2.3. Transverse Shear Locking Treatment

In the pure displacement-based finite element formulation of shells, employing the full quadrature rules leads to locking effects related to transverse shear strain energy values. These formulations give unacceptable results especially thickness values become smaller. To resolve the shear locking problem without reducing the quadrature rules, the ANS method is applied. The assumed transverse shear strains are based on the constant-linear interpolations of the compatible transverse shear strains $\varepsilon^{u}_{\xi\zeta}$ and $\varepsilon^{u}_{\eta\zeta}$ evaluated at the midpoints of the element edges. The local transverse shear strains are

$$\begin{Bmatrix}\overline{\varepsilon}^{u}_{xz}\\ \overline{\varepsilon}^{u}_{yz}\end{Bmatrix}=\begin{bmatrix}\overline{T}_{55}&\overline{T}_{56}\\ \overline{T}_{65}&\overline{T}_{66}\end{bmatrix}\begin{Bmatrix}\varepsilon^{ANS}_{\xi\zeta}\\ \varepsilon^{ANS}_{\eta\zeta}\end{Bmatrix} \tag{10}$$

in which the interpolated natural transverse shear strains are given by

Published By:
Blue Eyes Intelligence Engineering
and Sciences Publication (BEIESP)

$$\begin{Bmatrix}\varepsilon_{\xi\zeta}^{ANS}\\ \varepsilon_{\eta\zeta}^{ANS}\end{Bmatrix}=\begin{Bmatrix}(1-\eta)\varepsilon_{\xi\zeta}^{u}\big|_{(0,-1,0)}+(1+\eta)\varepsilon_{\xi\zeta}^{u}\big|_{(0,1,0)}\\ (1-\xi)\varepsilon_{\eta\zeta}^{u}\big|_{(-1,0,0)}+(1+\xi)\varepsilon_{\eta\zeta}^{u}\big|_{(1,0,0)}\end{Bmatrix} \quad (11)$$

2.4. Trapezoidal locking treatment

Trapezoidal locking occurs in the case of curved geometry. To resolve the locking effect from parasitic transverse normal strain, we interpolate the natural transverse normal strain at the nodal directors. That is,

$$\varepsilon_{\zeta\zeta}^{ANS}=N_1\varepsilon_{\zeta\zeta}^{u}\big|_{(-1,-1,0)}+N_2\varepsilon_{\zeta\zeta}^{u}\big|_{(1,-1,0)}+N_3\varepsilon_{\zeta\zeta}^{u}\big|_{(1,1,0)}+N_4\varepsilon_{\zeta\zeta}^{u}\big|_{(-1,1,0)} \quad (12)$$

and the local transverse normal strain is

$$\bar{\varepsilon}_{zz}^{u}=\bar{T}_{33}\varepsilon_{\zeta\zeta}^{ANS} \quad (13)$$

2.5. Membrane and thickness locking treatment

To avoid the membrane and the thickness locking problem in the solid shell formulations, the displacement-based strain field related to the membrane strains $(\varepsilon_{\xi\xi}^{u}, \varepsilon_{\eta\eta}^{u}, \varepsilon_{\xi\eta}^{u})$ and the transverse normal strain $\varepsilon_{\zeta\zeta}^{u}$ can be improved using the EAS method as following

$$\boldsymbol{\varepsilon}=\boldsymbol{\varepsilon}^{u}+\boldsymbol{\varepsilon}^{\alpha} \quad (14)$$

where $\boldsymbol{\varepsilon}$ is the improved strain field and $\boldsymbol{\varepsilon}^{\alpha}$ is the additive enhanced strain field. The additive enhanced strain field can be rewritten as

$$\boldsymbol{\varepsilon}^{\alpha}=\mathbf{B}^{\alpha}\boldsymbol{\alpha} \qquad \boldsymbol{\alpha}=[\alpha_1 \quad \alpha_2 \quad \cdots \quad \alpha_7]^{T} \quad (15)$$

where $\mathbf{B}^{\alpha}$ and is the EAS-based strain-displacement matrix, $\boldsymbol{\alpha}$ is vector of EAS variables. The matrix is given by

$$\mathbf{B}^{\alpha}=\begin{bmatrix}\xi & 0 & 0 & 0 & 0 & 0 & 0\\ 0 & \eta & 0 & 0 & 0 & 0 & 0\\ 0 & 0 & \zeta & \xi\zeta & \eta\zeta & 0 & 0\\ 0 & 0 & 0 & 0 & 0 & \xi & \eta\\ 0 & 0 & 0 & 0 & 0 & 0 & 0\\ 0 & 0 & 0 & 0 & 0 & 0 & 0\end{bmatrix} \quad (16)$$

In order to pass the membrane patch test and out-of-plane bending patch test, the bilinear polynomials for the transverse normal strain $\varepsilon_{\zeta\zeta}$ are necessary, i.e. the minimum number of EAS parameters for $\varepsilon_{\zeta\zeta}$ should be three. The enhanced strain field $\boldsymbol{\varepsilon}^{\alpha}$ in Eq. (16) is transformed into local coordinates by Eq. (9)

$$\bar{\boldsymbol{\varepsilon}}^{\alpha}=\frac{\det\mathbf{J}_0}{\det\mathbf{J}}\bar{\mathbf{T}}_0\boldsymbol{\varepsilon}^{\alpha}=\mathbf{B}^{\alpha}\boldsymbol{\alpha} \quad (17)$$

where $\bar{\mathbf{T}}_0$ are evaluated at the element center. The local membrane strains can be given in the form of

$$\begin{Bmatrix}\bar{\varepsilon}_{xx}^{u}\\ \bar{\varepsilon}_{yy}^{u}\\ \bar{\varepsilon}_{xy}^{u}\end{Bmatrix}=\begin{bmatrix}\bar{T}_{11} & \bar{T}_{12} & \bar{T}_{14}\\ \bar{T}_{21} & \bar{T}_{22} & \bar{T}_{24}\\ \bar{T}_{41} & \bar{T}_{42} & \bar{T}_{44}\end{bmatrix}\begin{Bmatrix}\varepsilon_{\xi\xi}^{u}\\ \varepsilon_{\eta\eta}^{u}\\ \varepsilon_{\xi\eta}^{u}\end{Bmatrix} \quad (18)$$

2.6. The Solution Method

The Newmark's method can be used to solve equation of motion of structures in dynamic analyses. Equation of motion of structure is given by

$$\mathbf{M}\ddot{\mathbf{u}}+\mathbf{C}\dot{\mathbf{u}}+\mathbf{K}\mathbf{u}=\mathbf{R} \quad (19)$$

here **M**, **C** and **K** denote mass, damping and stiffness matrices respectively.; $\mathbf{u}$, $\dot{\mathbf{u}}$ and $\ddot{\mathbf{u}}$ also denotes displacement, velocity and acceleration vectors; and **R** shows external forces.

A brief algorithm for the Newmark's method is given in the following.

1. **K , M** and **C** matrices of the system are calculated
2. Initial conditions for $\mathbf{u}$, $\dot{\mathbf{u}}$ and $\ddot{\mathbf{u}}$ are applied
3. Time increment Δt, parameters γ and β are selected to determine integration constants as follows

$$\gamma \geq 0.50; \quad \beta \geq 0.25(0.50+\gamma)^2$$

$$a_0=\frac{1}{\beta\Delta t^2}; \quad a_1=\frac{\gamma}{\beta\Delta t}; \quad a_2=\frac{1}{\beta\Delta t};$$

$$a_3=\frac{1}{2\beta}-1; \quad a_4=\frac{\gamma}{\beta}-1;$$

$$a_5=\frac{\Delta t}{2}\left(\frac{\gamma}{\beta}-2\right); \quad a_6=\Delta t(1-\gamma); \quad a_7=\gamma\Delta t;$$

4. Effective stiffness matrix $\hat{\mathbf{K}}$ is obtained

$$\hat{\mathbf{K}}=\mathbf{K}+a_0\mathbf{M}+a_1\mathbf{C} \quad (20)$$

5. Effective load vector $\hat{\mathbf{R}}_{n+1}$ is determined at time increment n+1

$$\hat{\mathbf{R}}_{n+1}=\mathbf{R}_{n+1}+\mathbf{M}(a_0\mathbf{u}_n+a_2\dot{\mathbf{u}}_n+a_3\ddot{\mathbf{u}}_n)+\mathbf{C}(a_1\mathbf{u}_n+a_4\dot{\mathbf{u}}_n+a_5\ddot{\mathbf{u}}_n) \quad (21)$$

Published By:
Blue Eyes Intelligence Engineering
and Sciences Publication (BEIESP)

6. Displacement vector $\mathbf{u}_{n+1}$ and incremental displacement vector $\Delta\mathbf{u}$ are calculated at time increment n+1

$$\mathbf{u}_{n+1} = \hat{\mathbf{R}}_{n+1}\,\hat{\mathbf{K}}^{-1} \quad (22)$$

$$\Delta\mathbf{u} = \mathbf{u}_{n+1} - \mathbf{u}_n \quad (23)$$

7. Following vectors are calculated at time increment n+1

$$\ddot{\mathbf{u}}_{n+1} = a_0\,\Delta\mathbf{u} - a_2\,\dot{\mathbf{u}}_n - a_3\,\ddot{\mathbf{u}}_n \quad (24)$$

$$\dot{\mathbf{u}}_{n+1} = \dot{\mathbf{u}}_n + a_6\,\ddot{\mathbf{u}}_n + a_7\,\ddot{\mathbf{u}}_{n+1} \quad (25)$$

$$\mathbf{u}_{n+1} = \mathbf{u}_n + \Delta\mathbf{u} \quad (26)$$

8. Time increment is updated as $n = n + 1$ and returned to step 6 [18-20].

III. NUMERICAL EXAMPLE

The element stiffness matrix is computed numerically using a 2×2×2 Gauss integration scheme. Most of the results presented here are compared with solutions of ANSYS SHELL63 element.

3.1. A Cantilever Subjected to End Shear Force

A cantilever is subjected to an end shear step force F, shown in Figure 2. The problem is examined using 20x1 enhanced solid-shell elements. Time step size and mass density is chosen as $2.5\text{x}10^{-4}$ and $7.85\text{x}10^{-9}$, respectively. Figure 3 plots the vertical end displacements of present and SHELL63 element results. The differences between two analyses are almost indistinguishable.

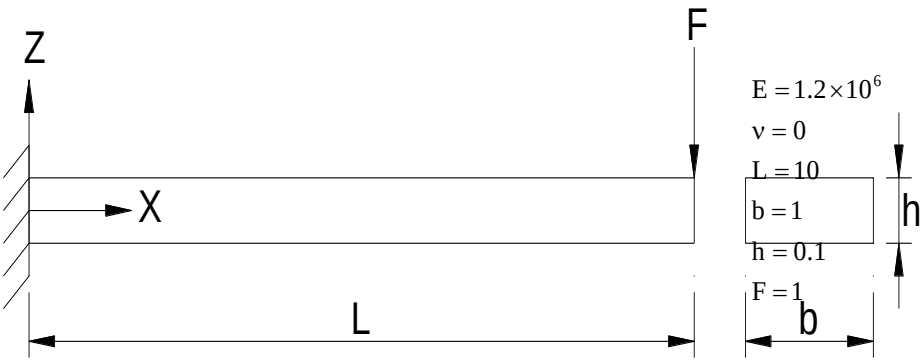

Figure 2. Cantilever subjected to end shear step force

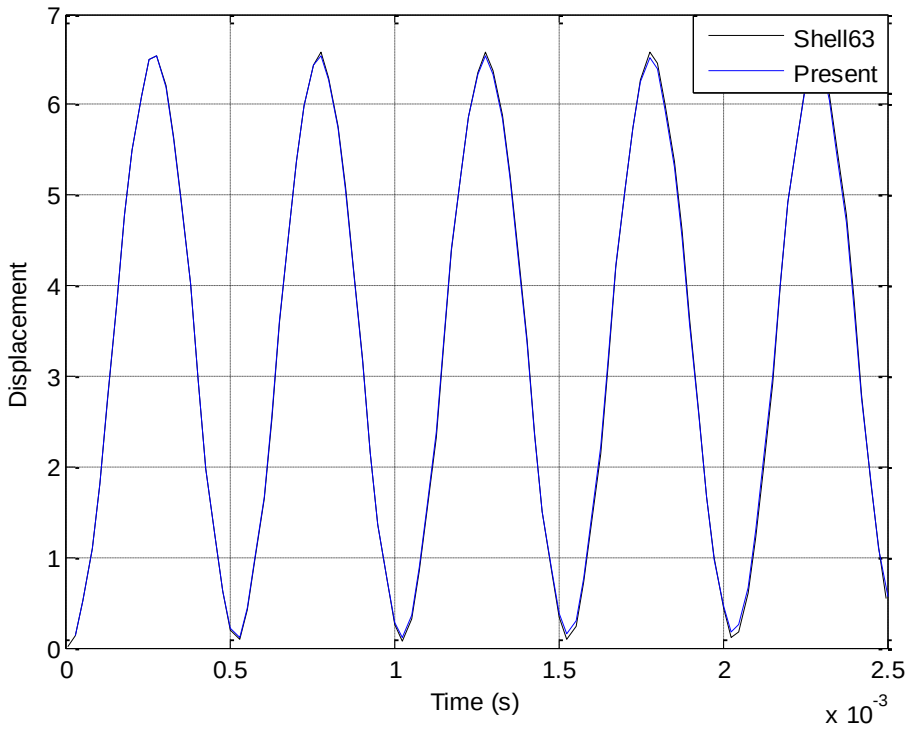

Figure 3. Time–displacement curves for cantilever subjected to end shear step force

Published By:
Blue Eyes Intelligence Engineering
and Sciences Publication (BEIESP)

3.2. Hinged Semi-Cylindrical Roof

A hinged semi-cylindrical roof shown in Fig 4, the straight edges are hinged and immovable while the curved edges are free.

The structure is modeled with 8x8 enhanced solid-shell elements on one quarter of its surface and with two elements in thickness direction. We investigate dynamic behavior of the cylindrical shell under a step force F=1000. Time step size and mass density is chosen as 2.5x10-4 and 7.85x10-9, respectively. The vertical displacements of point A is given in Figure 5 and compared with SHELL63 element solutions. A very good agreement between the solutions along the entire time–displacement path is noticeable.

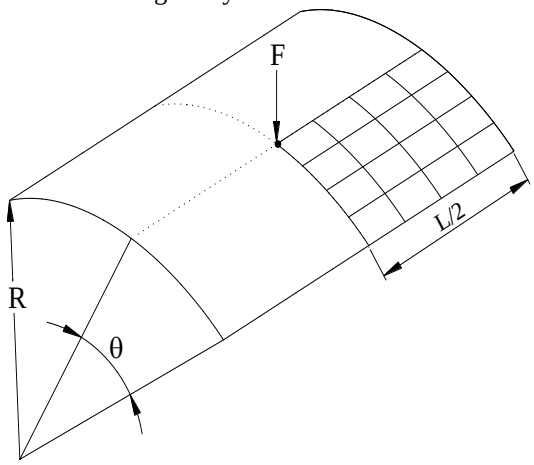

$E = 3102.75$

$\nu = 0.3$

$R = 2540$

$L = 508$

$h = 12.7$ *or*

$h = 6.35$

$\theta = 0.1$

Figure 4. Hinged semi-cylindrical roof subjected to a central point load.

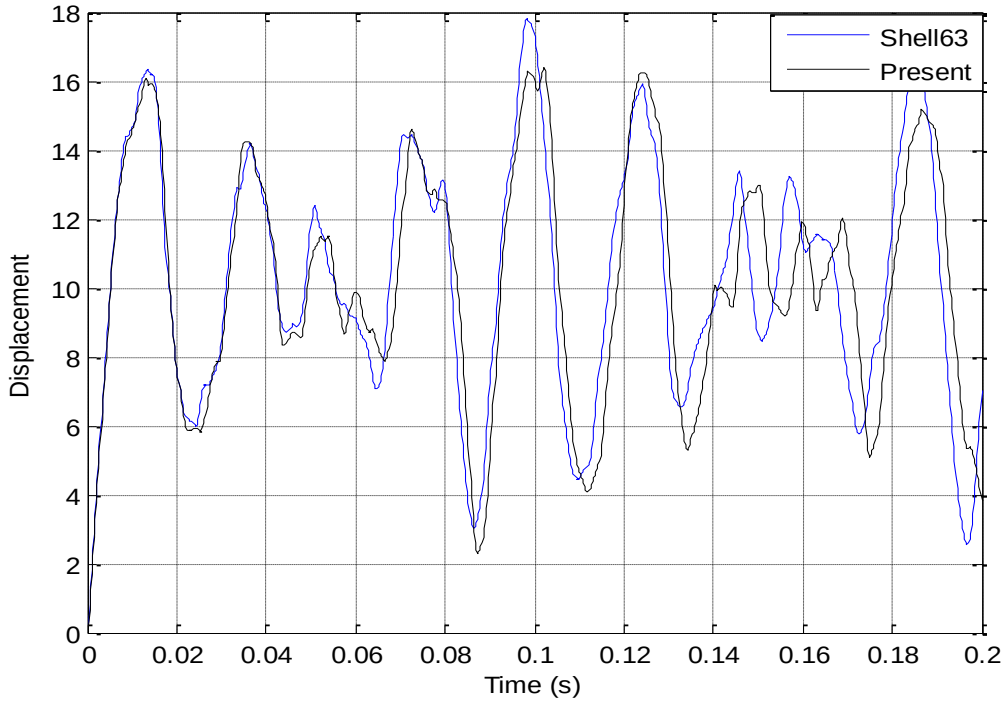

Figure 5. Time–displacement curves for the hinged semi-cylindrical roof

IV. CONCLUSIONS

Dynamic analysis of some structures are performed using a 8-node solid-shell element. The ANS and the EAS approaches were used to alleviate the locking problems. Thus, the element is nearly locking free. The governing equations were solved employing the Newmark's integration technique. Several benchmark problems are solved to demonstrate the efficiency of the element.

REFERENCES

1. Polat, C., & Calayir, Y. (2010). Nonlinear static and dynamic analysis of shells of revolution. Mechanics Research Communications, 37(2), 205-209.
2. Hauptmann, R., Schweizerhof, K., 1998. A systematic development of 'solid-shell' element formulations for linear and non-linear analyses employing only displacement degrees of freedom. International Journal for Numerical Methods in Engineering 42, 49-69.

Published By:
Blue Eyes Intelligence Engineering and Sciences Publication (BEIESP)

3. Hauptmann, R., Scheizerhof, K., Doll, S., 2000. Extension of the "solid-shell" concept for application to large elastic and large elastoplastic deformations. International Journal for Numerical Methods in Engineering 49, 1121-1141.
4. Sze, KY., Yao, LQ., 2000. A hybrid stress ANS solid-shell element and its generalization for smart structure modelling. Part I: solid-shell element formulation. International Journal of Numerical Methods in Engineering 48, 545-564.
5. Sze, KY., Yao, LQ., Yi, S., 2000. A hybrid stress ANS solid-shell element and its generalization for smart structure modelling. Part II: smart structure modelling. International Journal of Numerical Methods in Engineering 48, 565-582.
6. Harnau, M., Schweizerhof, K., 2002. About linear and quadratic "solid-shell" elements at large deformations. Computers and Structures 80, 805-817.
7. Vu-Quoc, L., Tan, XG., 2003. Optimal solid shells for non-linear analyses of multilayer composites. I. Statics. Computer Methods in Applied Mechanics and Engineering 192, 975-1016.
8. Sousa, RJA., Cardoso, RPR., Fontes Valente, RA., Yoon, YW., Gracio, JJ., Natal Jorge, RM., 2004. A new one-point quadrature enhanced assumed strain (eas) solid-shell element with multiple integration points along thickness- part 1: geometrically linear applications. International Journal for Numerical Methods in Engineering 62, 952-977.
9. Tan, XG., Vu-Quoc, L., 2005. Optimal solid shell element for large deformable composite structures with piezoelectric layers and active vibration control. International Journal of Numerical Methods in Engineering 64, 1981-2013.
10. Sousa, RJA., Cardoso, RPR., Valente, RAF., Yoon, JW., Gracio, JJ., Jorge, RMN., 2006. A new one-point quadrature Enhanced Assumed Strain solid-shell element with multiple integration points along thickness Part II – Nonlinear Applications, International Journal of Numerical Methods in Engineering 67, 160-188.
11. Zienkiewicz, OC., Taylor, RL., Too, JM., 1971. Reduced integration techniques in finite element method. International Journal for Numerical Methods in Engineering 3, 275-290.
12. Hughes, TJR., Cohen, M., Haroun, M., 1978. Reduced and selective integration techniques in the finite element analysis of plates. Nuclear Engineering and Design 46, 203-222.
13. Bucalem, ML., Bathe, KJ., 1993. Higher-order MITC general shell elements. International Journal for Numerical Methods in Engineering 36, 3729-3754.
14. Andelfinger, U., Ramm, E., 1993. EAS-elements for two-dimensional, three-dimensional, plate and shell structures and their equivalence to HR-elements. International Journal for Numerical Methods in Engineering 36, 1311-1337.
15. Polat, C. (2010). Co-rotational formulation of a solid-shell element utilizing the ANS and EAS methods. Journal of Theoretical and Applied Mechanics, 48(3), 771-788.
16. Polat, C. (2010). An assessment of a co-rotational EAS brick element. Latin American Journal of Solids and Structures, 7(1), 77-89.
17. Valente, RAF., 2004. Developments on shell and solid-shell finite elements technology in nonlinear continuum mechanics. Ph.D. Thesis, University of Porto, Portugal.
18. 104. Calayır, Y. and Polat, C., 2002, Çok Katlı Düzlem Çerçevelerin P-Delta Etkisi Dikkate Alınarak Deprem Analizi, Balıkesir Üniversitesi, IV. Mühendislik-Mimarlık Sempozyumu, 531-540.
19. Calayır, Y. ve Polat, C., 2002, An Iterative Approach for Seismic Analysis of Multistory Plane Frames Including P-Delta Effects, Symposium Proc. CREATING THE FUTURE 2nd FAE International Symposium, 209-214, Gemikonagı, TRNC.
20. Bathe, K. J., 1976, Numerical Methods in Finite Element Analysis, Prentice-Hall, Englewood Cliffs, 528p.

Published By:
Blue Eyes Intelligence Engineering and Sciences Publication (BEIESP)